Applied Thermal Engineering 198 (2021) 117469

Contents lists available at ScienceDirect

Applied Thermal Engineering

journal homepage: www.elsevier.com/locate/apthermeng

Optimal control of fan coil battery air and water flow rates requiring minimal on-line measurements

Kilian Edwards [a], Mattia De Rosa [b,c], Donal P. Finn [a,c,*]

[a] School of Mechanical and Materials Engineering, University College Dublin, Belfield, Dublin 4, Ireland
[b] Universitá degli Studi di Sassari, Via Vienna 2, Sassari, Italy
[c] UCD Energy Institute, University College Dublin, Belfield, Dublin 4, Ireland

ARTICLE INFO

Keywords:
Optimal control
Buildings
Fan coil
Energy efficiency
Thermal comfort

ABSTRACT

Fan coil units are widely used in air-conditioning systems for heating and cooling of commercial buildings. Control - capable of achieving better operational efficiencies and at the same time, guarantying thermal comfort - is paramount in order to achieve optimal operation. The present paper presents a novel generalised control strategy, requiring only minimal input data, for optimising fan speed in order to reduce. Different control models are implemented to predict fan coil capacities and associated total power consumption. The developed strategy has been compared to fixed speed and benchmark fan speed control strategies, using both a steady state and a quasi-steady state algorithm, for various building loads. Results show average reduction in fan coil battery power consumption of 34% and 43% in heating and cooling mode respectively, when the optimal control is compared to fixed fan speed settings. Savings between 4.9% and 9.1% can be achieved by the control algorithms if compared to the benchmark fan speed control strategies.

1. Introduction

The building sector is responsible for about 40% of the overall energy consumption and 36% of CO2 emissions worldwide. Consequently, a strong interest in implementing energy efficiency measures in buildings has been a priority in recent years. As a case in point, the European Union (EU) has introduced several requirements for new and existing buildings through the "*Energy Performance of Building Directive*" (EPBD) [1] and the "*Energy Efficiency Directive*" [2]. In order to fulfil the EPBD requirements and, at the same time, to ensure the thermal comfort for occupants, the optimisation of all possible aspects - e.g., envelope, heating/cooling system components, control criteria, etc. - has to be pursued commencing with the earliest stage of the design cycle [3].

In this context, HVAC (heating, ventilation and air conditioning) systems account for more than half of overall building energy consumption [4], and they play a paramount role both in ensuring occupant comfort and in offering opportunities to increase energy efficiency. Fan coil units (FCU) are widely used as air-conditioning devices in particular, for large buildings with central heating/cooling systems, where local control is required (e.g., hotels, commercial buildings, etc.). The global air conditioning market reported annual sales of more than 110 million units in 2018, with room units accounting for 87% of that value [5]. The drive energy required by these systems is an important factor in determining the overall system efficiency, since a reduction in performance may be observed at partial loads due to unnecessary pumping or fan power [6]. Therefore, the power consumed by fan coils, in addition to other factors such as control of thermal comfort, is an important operational constraint when implementing control strategies. Moreover, the development of a network control platform is critical in order to achieve meaningful energy savings, in particular for multi-zone HVAC units [7], as well as for implementing demand-side management and demand response programs [8].

Methods for optimising water and air flow rates to reduce associated FCU motive power consumption have been researched for large once-off custom installations [7,9–11]. In these cases, a significant number of on-line power and temperature measurements are required for media flow rate optimisation. Due to the nonlinear relationship between water/air flow rate and fan coil power/capacity [12], optimal set-points are not easily obtained using available system measurements, such as fluid temperatures and flow rates only. Moreover, the overall performance of a system can be strongly influenced by the efficiency of single components, especially if frequent partial load conditions occur [3]. For such conditions, control strategies that take into account the component performance optimisation from a system perspective, with the aim of maximising the overall system performance, are needed. Relatively few

* Corresponding author at: School of Mechanical and Materials Engineering, University College Dublin, Belfield, Dublin 4, Ireland.
E-mail addresses: mderosa@uniss.it (M. De Rosa), donal.finn@ucd.ie (D.P. Finn).

https://doi.org/10.1016/j.applthermaleng.2021.117469
Received 1 April 2020; Received in revised form 15 July 2021; Accepted 16 August 2021
Available online 1 September 2021

Nomenclature

Δ	Temperature difference, °C
$\dot{m}$	Mass flow rate, kg s^{-1}
a	Air
AHU	Air handling unit
C	Heat capacity rate, kJ, kWh
C_1, C_2, C_3, C_4, C_5	Pump correlation constants
C_4, C_5	Fan coil water mass flow constants
C_p	Specific Heat, J kg^{-1} K^{-1}
d	design
F	Correlation function
f	Fluid
fc	Fan coils
FCU	Fan coil unit
GSHP	Ground source heat pump
HVAC	Heating, ventilation and air conditioning
in	Inlet
o	Outlet
P	Power, KW
Q	Thermal Power, KW
r	real, KW
T	Temperature, °C
w	Water
x	Change in water flow rate
y	Change in fan coil capacity

studies have focused on optimal control using minimal input data for small or medium capacity FCU systems working at partial loads.

In order to address this research gap, the present paper describes the development and testing of a novel generalised control strategy for minimising power consumption of a fan coil battery at part load, requiring only minimal available input data. The following sections outline a literature review on fan coil unit control (Section 1.1 and a summary of the motivation of the present work 1.2.

1.1. Overview of control in fan coil units

Typically, the primary objective of emitter terminal units is to maintain thermal comfort within a conditioned space either through control of air temperature or radiant heat or both. For FCUs specifically, from a control perspective, the objective is generally to maintain the zone air temperature within a specified bandwidth by adopting a rule-based approach. This method is based on limiting the variation of specific design parameters - such as, internal temperature, fan speed, water temperature, etc. - within a range around a predetermined set point. Typically, a set of at least four online measurements would be required to control fan coil batteries in these conventional strategies (i.e., fan power, pump power, fan coil water inlet temperature and fan coil inlet air temperature) [13,14].

Generally, maintaining the zone set-point air temperature can be challenging as the dynamic response of the building indoor air temperature is slower than that one associated with the FCU hydronic system. This can present difficulties when implementing variable speed direct feedback or predictive control. In addition to comfort control, the power consumed by fan coils can constitute a not insignificant proportion of the total system power demand. Moreover, controlling the internal water circuit to maintain the air temperature at a particular set point can have a negative effect on efficiency at partial load [15], despite the associated water thermal inertia which may offer stability benefits.

In order to reduce the power consumed by terminal units (fan coils), while operating at part load, the delivered capacity can be modulated using direct feedback control to maintain the room temperature [16]. Dedicated circulation pumps or 3-way valves [17] are often necessary, as optimal water flow rate to the terminal units is typically different from the primary circuit optimal flow rate. By controlling the differential pressure at the circulation pumps, the pressure drop introduced by an air handling unit (AHU) valve control can be reduced to improve efficiency [9,18].

Fan speed may also be controlled to modulate the delivered capacity using either multi-speed or variable speed controls [19]. However, manual selection of fan speed is often implemented. A further reduction in power consumption may be realised by controlling both air and water flow rate: fan speed can be set to increase or decrease when defined water valve opening set-points are exceeded. For instance, Tianyi et al. [10] modulated fan speed and water valve duty ratio to reduce power consumption, while maintaining room temperature at a specified set-point, using a fuzzy control method. Another method of optimising air and water flow rates is through matching air side and water side temperature differences. With this approach, air and water heat capacity rates are set equal: the fluid with the minimum heat capacity rate C_{min} experiences a greater change in temperature than that with maximum heat capacity rate C_{max} and therefore has a constraining effect on the unit heat transfer capacity [20]. Generally, it is possible to reduce the value of C_{max}, through flow rate control, without a significant loss in capacity [21].

Typically, the type of controls for fan coil batteries can be summarised as follows:

- *Air flow rate control*: Standard fan coil control prescribes that fan speed should be set manually in each zone in order to ensure occupant comfort, as personal control of air flow is usually desired, and to reduce excessive changes in fan speed in order to avoid noise issues or other user considerations. Variable air flow can also be modulated using a bypass damper rather than direct fan speed control [22]. For multi-speed fan coil units, fan speed can be controlled using room temperature bandwidth, where the fan speed is increased when the current setting is unable to maintain the room temperature at the specified set-point [10].
- *Water temperature and flow control*: Water temperature set-point influences both the heat pump and FCU performance. In the case of single FCUs, the water temperature can be adjusted by controlling the return set-point. For a system with multiple fan coils, the water temperature can be controlled locally through the use of bypass lines that accommodate mixing inlet and return water flows. Ideally the water temperature set-point must be sufficient to ensure the load delivery, while maximising heat pump performance, which is highly dependent on temperature (e.g., decreasing the supply temperature, in heating mode, from 55 °C to 35 °C can increase the SPF by up to 40% [13]). Generally, the standard water temperature set-point control dictates that, as the building load decreases, the supply temperature should be lowered in heating and raised in cooling. The supply temperature set-point is reset according to a curve relating supply and ambient temperatures, based on the design ambient temperature and the heating/cooling delivery system type [23]. The benefits of water temperature control are related to an improvement in the heat pump performance rather than a reduction in pump or fan power. The water flow rate through a fan coil can be modulated using either valve control or direct pump control. Alternatively, the flow rate can be continuously modulated using PID valve control [24,25]. Fahlén et al. [26] demonstrated that variable water temperature control is generally favoured to water flow control.
- *Fan coil optimisation control*: While studies have researched air/water flow rate and water temperature controls independently as a form of

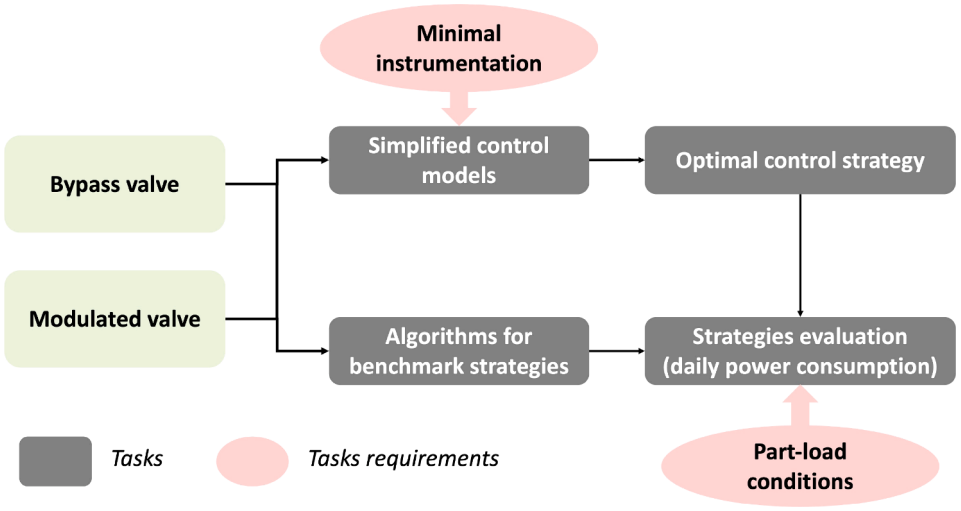

Fig. 1. Summary of the methodology adopted.

capacity control, a reduction in power consumption may be obtained from controlling two or more of these variables. An increase in fan coil capacity with a change in water flow, air flow or water temperature also results in an increase in pump power, fan power or a degradation in heat pump performance. The optimal set-points are not easily obtained due to the non-linear relationships between power and capacity for each of these variables [12]. To ensure stable and robust controls, one variable is commonly modulated using direct feedback control, to match the required load, while the other can then be updated based on the operating set-point of the first variable. A commonly cited method of optimising air and water flow rates is matching air side and water side temperature differences [20]. Using this method, the air and water heat capacity rates are made equal. The fluid with the minimum heat capacity rate (C_{min}) experiences a much greater change in temperature than the one with maximum heat capacity rate (C_{max}) and, therefore exerts the dominant influence on heat transfer. It is therefore possible to reduce the value of C_{max}, through flow rate control, without a significant loss in capacity. For fan coil systems, C_{max} is normally related to the water side, with a capacity ratio C_{max}/C_{min} of 1.5–2 [21]. This suggests that the water flow rate can be reduced by up to half its value, resulting in a decreased pumping power, without a significant loss in capacity. Markusson [27] showed that the optimum water flow rate is 25% of the design value when the air flow rate was set to its design flow. Therefore, controlling the air and water flow rate to equate the heat capacity values can reduce overall power of the fan coil battery. Starting from this concept, a new control strategy, based on a reduced number of input parameters to limit the acquisition system requirements, has been developed and tested, as described in the following sections.

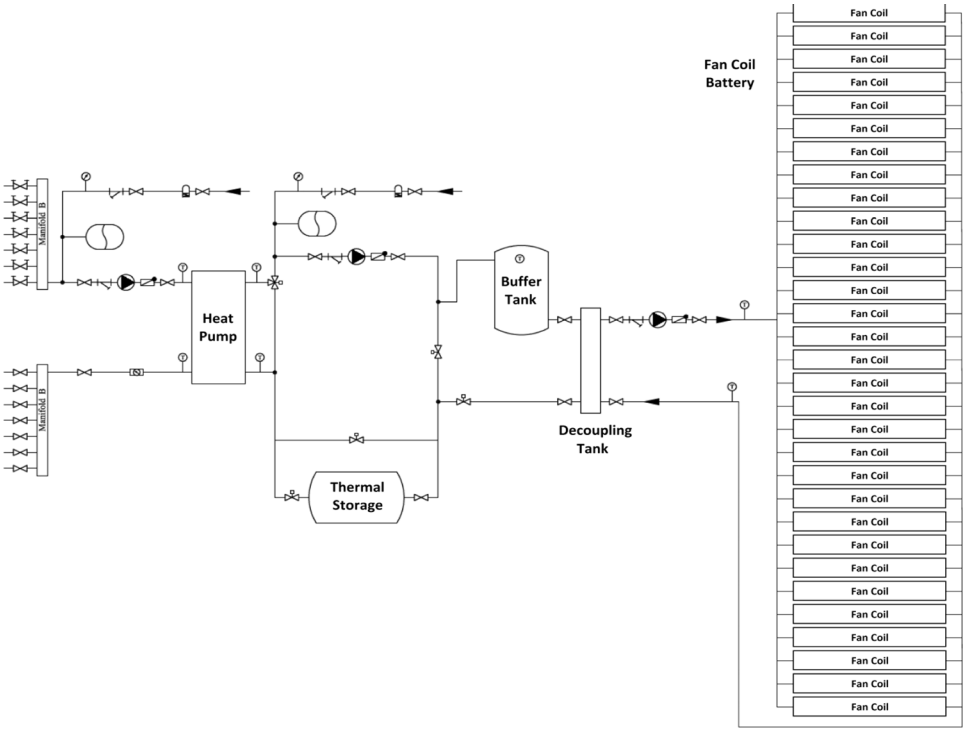

Fig. 2. GSHP system of the demonstrator site in Coimbra, Portugal [28].

1.2. Motivation and paper outline

The present paper describes a novel generalised control strategy for fan coils units requiring only minimal input data, which is aimed at minimising power consumption while maintaining the operation within the zone temperature set-points and bandwidth. The key contribution of the proposed approach is twofold:

- the need for reduced data measurements - both in terms of the number of measurements, the type of measurements and the frequency of measurements. For HVAC system control, reliability of measurements is a key issue, therefore any proposed contribution that minimises the number and the frequency of measurements, coupled with simplifying the measurement approach has the potential to enhance and deliver improved control methods, and,
- the development of a control strategy based on a new correlation exploiting minimal data set - namely, water and air inlet temperatures and available fan coil battery nominal design data - capable of optimising the fan coil battery operating conditions to reduce its energy consumption while maintaining the indoor thermal conditions.

The new correlations are tested on a real experimental test facility consisting of a geothermal heat pump system for heating and cooling of an office building. The strategy is evaluated and compared to benchmark strategies, using a simulation model, utilising both steady state and quasi-steady state modelling conditions, within a whole building analysis environment. The novelty of the approach in the current research is that it exploits readily available design data for each fan coil within a fan battery system, which is combined with minimal operational data, so as to set the optimal fan speed for each fan coil unit in a fan coil battery system, thereby minimising fan power consumption while satisfying the necessary thermal demand for each zone.

Despite the specific nature of the application analysed in the present paper, the developed strategy has the potential to be adapted to different system designs where fan coil batteries are used as emitters, given the availability of design data and online measurements of air and water inlet temperatures.

2. Methodology

A control strategy to minimise the fan coil battery power consumption through the control of air and water flow rates has been developed. A reduced number of input parameters are required: (i) the design data of both fan coil and circulation pump, and (ii) the real time fan speed and fan coil water flow rate. The overall methodology is summarised in Fig. 1.

The control strategy was implemented in a simulation model to characterise the fan coil battery of a ground-source heat pump (GSHP) system installed to service one floor of a public building in Coimbra (Portugal), a demonstration site of the EU FP7 GROUNDMED project [28,29]. The GSHP system, shown in Fig. 2, consists of a total of 31 fan coils distributed over 20 zones. A decoupling tank is present in the system, separating flow between the heat pump and the terminal units, allowing the assumption of considering the fan coil battery in isolation. Built-in water flow control is utilised for each fan coil through the use of 3-way valves, modulated using a PID control, to maintain the room air temperature at a predetermined set-point. The fan speed setting can be selected from three set values. More information about the experimental facility can be found in Carvalho et al. [29].

Co-simulation between Matlab and EnergyPlus was not used in the current work. Simulation models were developed separately for each component (circulation pump, fan coils and building) and then, combined into a system model which was implemented in the MATLAB environment, while a full building simulation model, developed in EnergyPlus, was utilised to calculate the zone loads over the course of a daily simulation. As the dimensions and occupancy of each zone were accounted for in the EnergyPlus model, the load varies for each zone. These zone loads act as boundary conditions for the control optimisation routines which were implemented in Matlab. From this, a full Matlab was developed to describe the fraction of total building load that each zone represents and all components of the building energy system. This model is utilised to calculate the zone loads and to implement the control strategies, (described in Section 2.3), for each simulation time step of 5 s. Further details of the simulation models and control strategies are provided in the subsequent sections.

Table 1
Building model part load and maximum capacity (heating/cooling).

Heating/Cooling	Max Partial Load	Power [kW]
H1/C1	0.1	7/6
H2/C2	0.2	14/13
H3/C3	0.3	21/19
H4/C4	0.4	28/25
H5/C5	0.5	35/32
H6/C6	0.6	42/38
H7/C7	0.7	49/44
H8/C8	0.8	56/51
H9/C9	0.9	63/57
H10/C10	1.0	70/64

2.1. Simulation models

The building simulation demand model was developed using experimental data from two representative two sample days, one in heating mode and one in cooling mode. The selected days represent the range of possible average daily part loads in heating and cooling mode. For each of the selected days, experimental data at a 1 min increment was obtained, as described in Edwards and Finn [30]. The simulation model utilised in the current work is described in Edwards and Finn [30], Corberan et al. [14], Montagud et al. [31], which summarise the development and validation of the simulation model.

Part loads were determined at the end of each on/off heat pump cycle using this data. For each cycle, the maximum part load (see Table 1) was used to determine the building load over the specified period. Using the power profiles from the two sample days, a series of building load profiles were created with peak daily part loads ranging from 0.1 to 1.0 in increments of 0.1. These load profiles are labelled H1 to H10 and C1 to C10 for heating and cooling, respectively. Table 1 reports the maximum capacities for both heating and cooling at each partial load considered, while the correspondent profiles with partial loads of 0.1, 0.5 and 1 are shown in Fig. 3.

The circulation pump on the building side operates with a built-in pressure control. For a selected differential pressure set-point, pump power vs water flow rate curves are available from the circulation pump data sheets. Using this data, a correlation was developed to express the pump power (P_p) as a function of water flow rate ($\dot{m}_w$), which takes the following form:

$$P_p = C_1 \dot{m}_w^{C_2} + C_3 \quad (1)$$

where C_1, C_2 and C_3 are constants. The fan coil units operate with a built-in water flow rate control to maintain the room air temperature at the set-point. This control is incorporated into the fan coil simulation model. It is assumed that the built-in control operates effectively - i.e., the water flow rate through the coil is always set to the value required to maintain the room temperature at the set-point. A fan coil simulation program available from the fan coil manufacturer, designed to simulate fan coil batteries using an iterative solution scheme, was utilised to generate fan coil capacity values over a range of fixed air and water flow rate combinations. Correlation curves were fitted to the simulated data points for each of the three fan speeds and for both fan coil unit types. As the fan coil capacity (Q_f) can be obtained from the zone load, the

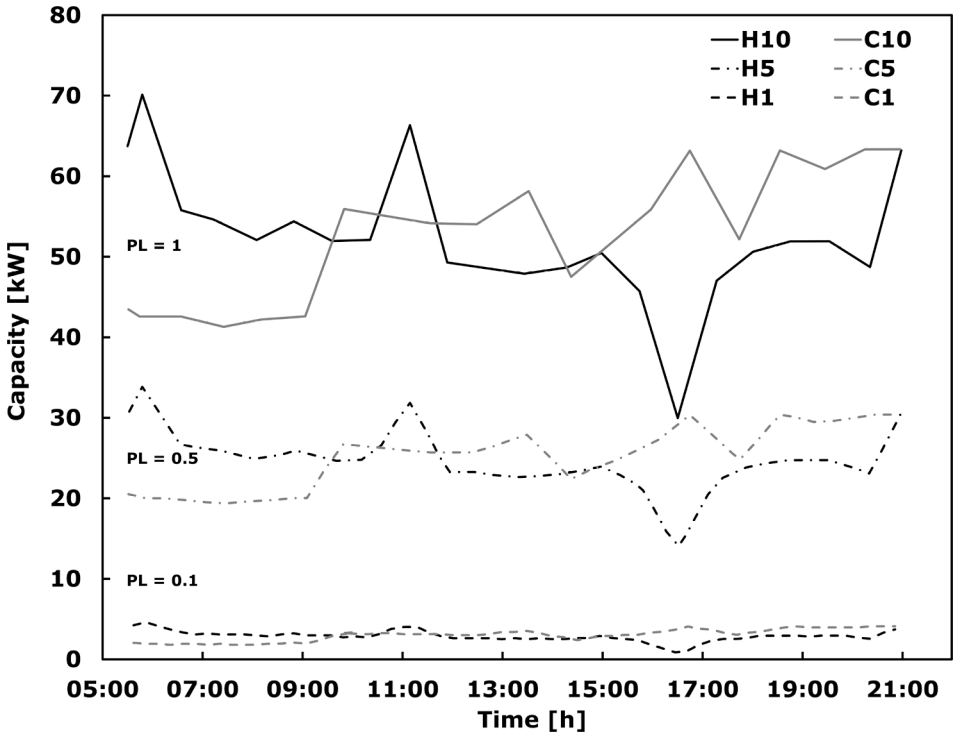

Fig. 3. Heating and cooling profiles for different part loads.

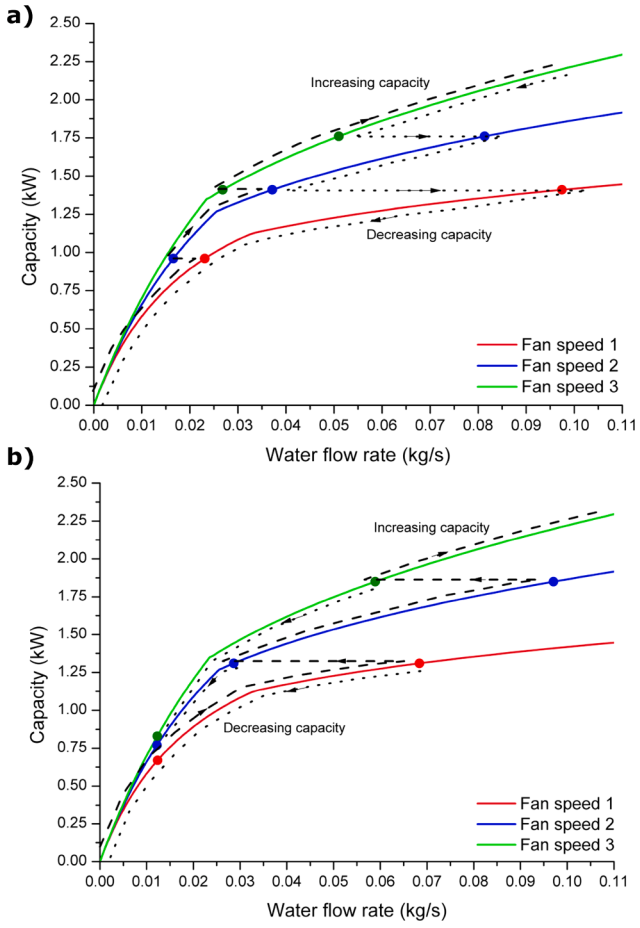

Fig. 4. Experimental fan coil units – Control operation. (a) Equating air and water heat capacity rate. (b) Design water flow control.

required fan coil water flow ($\dot{m}_{wf}$) for any zone is calculated as shown below:

$$\dot{m}_{wf} = \left[\frac{Q_f\left(T_{w,in,d} - T_{a,in,d}\right)}{C_4\left(T_{w,in} - T_{a,in}\right)}\right]^{C_5} \quad (2)$$

where C_4 and C_5 are constants, $T_{w,in,d}$ and $T_{a,in,d}$ are the nominal water and air inlet temperatures respectively, while $T_{w,in}$ and $T_{a,in}$ are the water and air inlet temperatures respectively.

Both Eq. 1 and 2 are based on regression fits provided by the respective manufacturers of the pump and fan units.

2.2. Benchmark strategies

Two benchmark control strategies were developed, for the purpose of comparison with the optimal control strategies developed in the current paper. These strategies are based on standard control principles described in the literature [21,32]. As the water flow rate through each fan coil is modulated using built-in PID control, the benchmark strategies operate by controlling fan speed based on current water flow rate set-point. The description of the benchmark strategies are reported below.

- *Equating air and water heat capacity rate ($C_{min} = C_{max}$)*: considering that the flow rate of the fluid with the minimum heat capacity rate (C_{min}) has a greater influence on delivered fan coil capacity than the fluid with the maximum heat capacity rate (C_{max}) [32], the first benchmark strategy was developed such that the fan speed is modulated in order to reduce the difference between water and air heat capacity rates (C_w and C_a). The objective of this strategy is to calculate the current C_w and C_a values, and for either, increase C_{min} or decrease C_{max}, depending on which is required in order to meet the criterion. A required increase or decrease in capacity can be detected from the change in water flow rate. The selected air and water flow rate set-points for increasing and decreasing capacity is shown in Fig. 4a. As the required capacity increases, the water flow rate

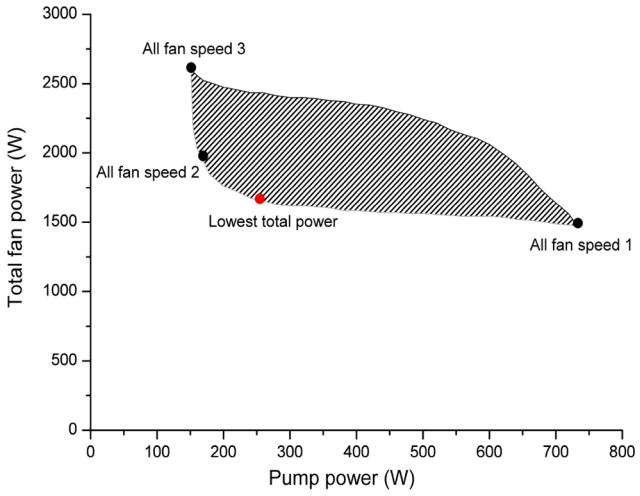

Fig. 5. Total fan power VS pump power and optimum working condition.

increases too. Once C_w surpasses C_a, the fan speed is increased. For decreasing capacity, and hence water flow rate, the fan speed is reduced when C_w drops below C_a.

- *Design water flow control*: the second benchmark strategy was developed with the aim of limiting excessive water flow rate, assuming the design fan coil water flow rate as an upper flow limit. The fan speed setting is increased when the water flow rate limit is exceeded. A lower water flow limit is also specified, selected as 10% of the design flow rate, deployed as a criterion to decrease the fan speed. Fig. 4b shows the change in fan speed for increasing and decreasing capacities.
- *Optimal air and water flow rate*: for a given supplied fan coil capacity, optimal air and water flow rates exist to minimise total power consumption. Considering the specific fan coil battery system tested, the water flow rate through each fan coil is modulated by means of a PID control, to maintain the room temperature in each zone at the selected set-point. Therefore, the total water flow rate in the system, and hence pumping power, is dependent on the flow rate through each individual fan coil. The optimal flow rates cannot be calculated for an individual fan coil but must be analysed on a system level, as the relationship between the change in water flow through one fan coil and the change in pump power will depend on the flow rate in all the other fan coils. Moreover, the combination of different fan speeds resulting in the minimum fan coil battery power consumption will depend on the capacity requirement of each zone. This represents an optimisation challenge due to the substantial number of possible fan speed combinations normally present. In the system analysed in the present paper, three possible fan speed set-points exist for each of the 31 fan coils. The optimal combination of fan speeds cannot be easily ascertained and will only result in the minimum total power for that specific set of zone loads. In order to obtain the relation between fan speeds and pump power, a series of fixed zone loads was selected as reference. For a set of fan speeds, the total fan and pump powers were calculated using the simulation model. Then this procedure was repeated for a large number of fan speed sets. Fig. 5 illustrates the pump power and total fan power for each set of simulated fan speed assignments. Fan speed sets with all speeds at values 1, 2 and 3 are highlighted, and the set resulting in the minimum total power is also indicated. The shaded area represents the fan and pump power for all other fan speed sets. When all fan speeds are at a value of 3, the largest fan power and lowest pump power are observed. Vice versa, the opposite occurs when all fan speeds are set at a value of 1. Generally, for fixed zone loads, an increase in fan speed results in a decrease in pump power. If the rate of decrease in pump power is larger than the rate of increase in fan power, a lower total power will be observed. The minimum total power is located at a point where the rate of change in the pump power is equal to the rate of change in total fan power. In this case, by operating at the optimal combination of fan speeds, the total power consumption can be reduced by 13%, 10% and 30%, when compared to fixed fan speeds of 1, 2 and 3 in all zones, respectively.

2.3. Optimal fan speed control strategy

A generalised control strategy was developed for determining optimal air and water flow rates, based on the GSHP system illustrated in Fig. 2. In order to predict optimal air/water flow rates for a given delivered capacity, a comparison of total power values (resulting from all possible air/water flow combinations) is required.

For this purpose, the estimation of the current delivered capacity for all air/water flow rate combinations is needed. Total power resulting from each of these options had to be estimated in order to select the minimum power air/water flow combination. The constraint of minimal availability of real-time measurements must be considered when estimating capacity and total power, in order to ensure the applicability of the strategy to different systems. If differential pressure control is implemented to modulate the pump speed, the pump power will be calculated for a given water flow rate at a specified pressure set point. A correlation, as per Eq. 1, relating pump power to water flow rate using the pump curves available from manufacturer data sheets, was then developed. The fan power can be taken directly from the fan coil data sheets for each fan speed setting. However, calculating the delivered capacity from measured air/water flow rates and inlet temperatures is not straightforward. A method of estimating the fan coil capacity is described here below.

2.3.1. Fan coil capacity estimation

Fan coil capacity does not vary linearly with water and air flow rate [12]. The relationship between capacity and fluid flow through a heat exchanger depends upon the fan coil unit design and dimensions, along with the flow rate of the other fluid. If the inlet/outlet temperature differences and flow rates on either the air or water side are measured, the fan coil thermal power (Q_{fc}) could be calculated as shown below:

$$Q_{fc} = \dot{m}_w c_{p,w}\left(T_{w,in} - T_{w,out}\right) = \dot{m}_a c_{p,a}\left(T_{a,out} - T_{a,in}\right) \tag{3}$$

where $\dot{m}_w$ and $c_{p,w}$ are the water mass flow rate and specific heat,$\dot{m}_a$ and $c_{p,a}$ are the air mass flow rate and specific heat, $T_{w,in}$ and $T_{w,out}$ are the water inlet/outlet temperatures ($T_{a,in}$ and $T_{a,out}$ are the air inlet/outlet temperatures.

While inlet air and water temperatures are often measured in building installations, the outlet temperatures are generally not recorded. Therefore, a new correlation has been developed in order to determine the fan coil capacity as a function of water and air inlet temperatures, knowing the fan coil design (nominal) parameter (subscript d). Similarly to the correlation developed by Markussonet al. [32], the new correlation expresses the change in fan coil capacity y (Eq. 4) as function of the change in water flow rate x (Eq. 5), assuming a fixed fan speed.

$$y = \frac{Q_r}{Q_d} \tag{4}$$

$$x = \frac{\dot{m}_r}{\dot{m}_d} \tag{5}$$

The resulting correlations for heating and cooling modes are reported in Eq. 6 and Eq. 7, while the methodology to derive them is described in Appendix A.

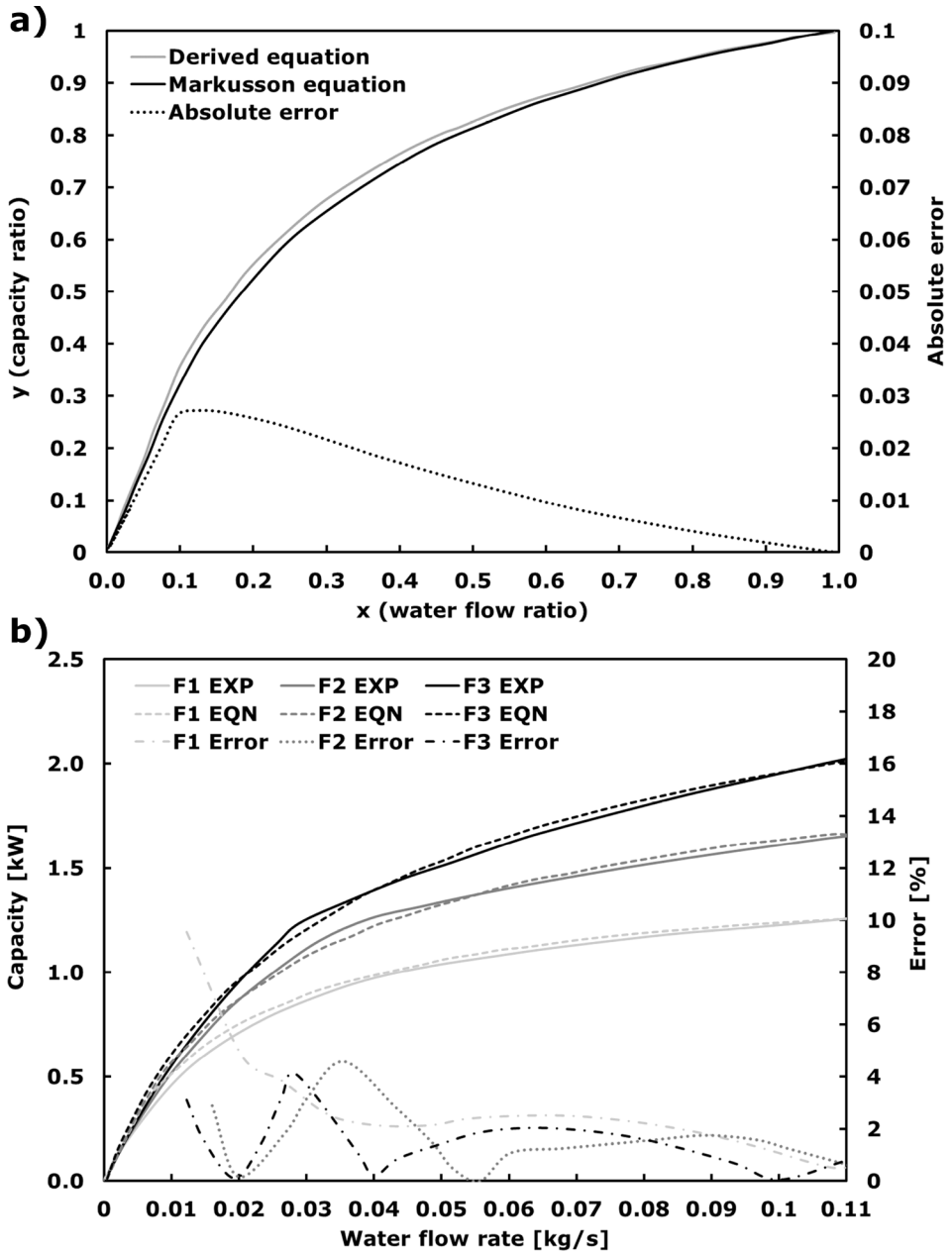

Fig. 6. (a) Comparison between the derived equations and Markusson's equation [32]. (b) Comparison between estimated and measured capacity values and error (in percentage) obtained for different water flow rates.

$$y = \frac{2F(x)\left(\frac{T_{w,in}}{\Theta_d} - \frac{T_{a,in}}{\Theta_d}\right)x}{2x + F(x)\left(\frac{\Delta T_{w,d}}{\Theta_d} + x\frac{\Delta T_{a,d}}{\Theta_d}\right)} \tag{6}$$

$$y = \frac{2F(x)\left(\frac{T_{a,in}}{\Theta_d} - \frac{T_{w,in}}{\Theta_d}\right)x}{2x + F(x)\left(\frac{\Delta T_{w,d}}{\Theta_d} + x\frac{\Delta T_{a,d}}{\Theta_d}\right)} \tag{7}$$

Eq. 6 and Eq. 7 refer to the fan coil nominal values which can be obtained from the fan coil data sheets: internal fan coil volume (V_f), fan coil pipe diameter (D_{pipe}), nominal inlet air and water temperatures ($T_{a,in}$ and $T_{w,in}$), nominal outlet water temperature (T_{w_out}), nominal air flow rate ($\dot{m}_a$) and fan coil capacity (Q_d). The required fan coil capacity (Q_r) from the calculated capacity ratio y and the nominal fan coil capacity (Q_d) adjusted on the measured inlet temperatures ($\Delta T_{in,r}$), as shown in the equation below:

$$Q_r = yQ_d\frac{\Delta T_{in,r}}{\Delta T_{in,d}} \tag{8}$$

2.3.2. Model verification and validation

The simulation models used in the current paper were developed in an incremental manner over a number of years, primarily within the context of the aforementioned GroundMed project [28]. Verification and validation of the models has been carried out at different incremental stages as follows: (i) at a heat pump level, (ii) at a building integrated HVAC system level, and (iii) at a fan coil level. Full details concerning the development and validation of the heat pump model can be found in Edwards and Finn [30], Corberan et al. [14], Montagud et al. [31]. Initially, preliminary models of the heat pump systems at a component level were developed using IMST-ART [33], and the associated model and validation is described in Corberan et al. [14]. Further

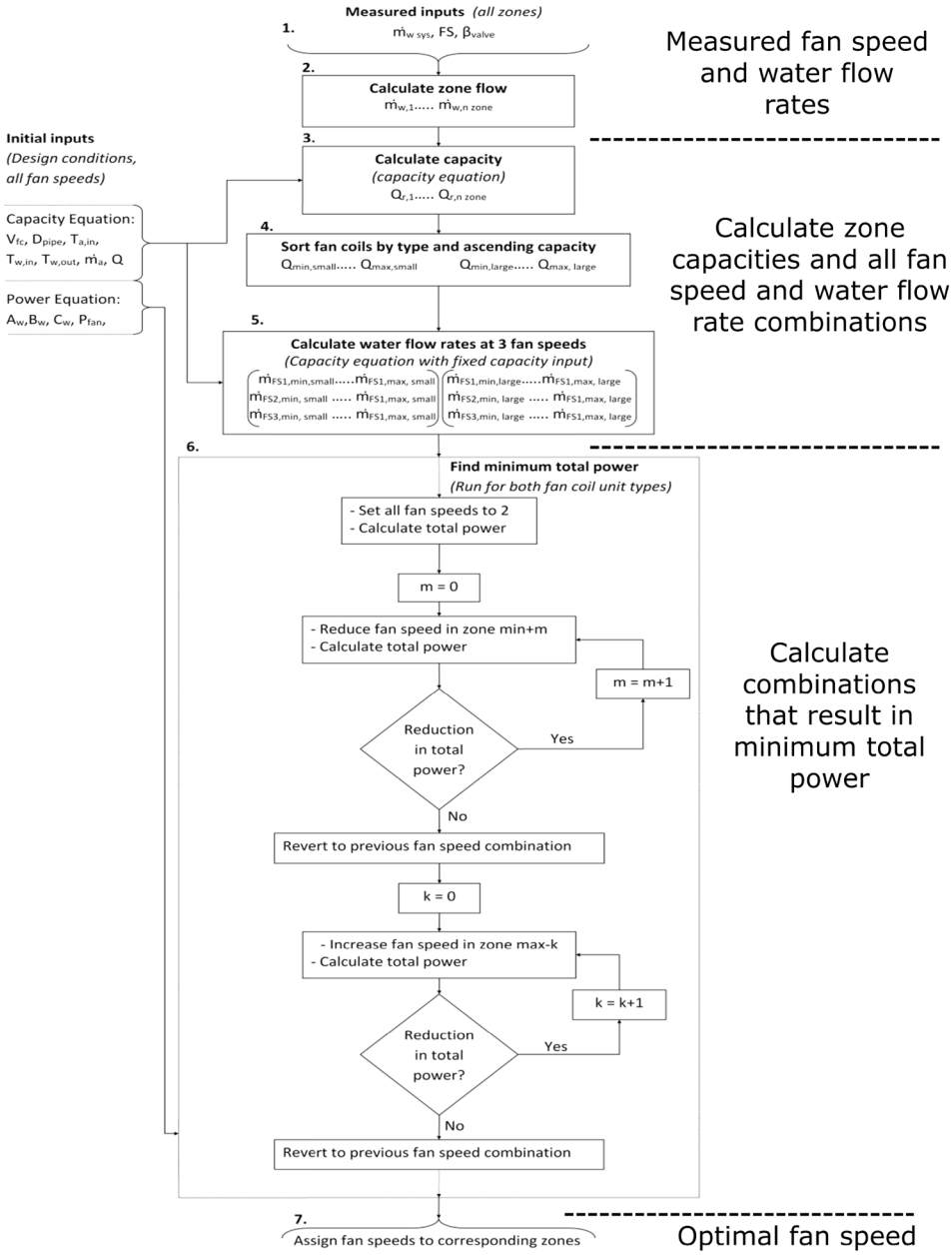

Fig. 7. Optimal fan speed control flow diagram.

model developments and relevant validations were carried out in a research laboratory, where mathematical models for different heat pump configurations (a single compressor system and a tandem compressor system operating in two modes) were compared with experimental data [34].

Commencing with these previous works, the present paper develops, validates and tests numerically a control approach for a fan coil battery based on a minimal measured data requirement and available nominal design data. As already explained in Section 2.3.1, Eqs. 6 and 7 - which underpin the approach described in the current work - are a modified form of those proposed by Markusson [27] (Eqs. A.1 and A.2) to account for the reduced measured data requirements. However, the two equation sets cannot be considered to be similar: all of the input data required for 6 and 7 can be obtained from the fan coil data sheets, with the exception of the ratio of the air to water side heat transfer coefficients and surface areas. Fig. 6a shows the comparison between the new correlation and the one derived by Markusson et al. [32] (Eq. A.1) for the fan coil units installed, where *x* and *y* represent the capacity (Eq. 4) and flow rate (Eq. 5) ratio. It is possible to observe that the predicted capacity ratio obtained by both equations are similar, with a maximum absolute error of 0.03 occurring at low flow rates.

The correlation was implemented in MATLAB and the simulated capacities were calculated over a range of water flow rates and fan speeds, adopting a fixed inlet air and water temperatures (25 °C and 9 °C respectively). Preliminary results were presented in Edwards and Finn [35]. Fig. 6b shows the comparison between the estimated fan coil capacity (calculated using Eq. 8) and the measured capacity of the fan coil unit. As this equation is defined for a fixed air flow rate, a separate equation is generated for each fan speed (F1, F2, F3). The comparison between the correlations and experimental data is shown in Fig. 6b, where it is possible to observe a good performance of the correlations for all air flow setting points at higher water flow rates. At low water flow rates, the difference between experimental and numerical data is more pronounced, especially for the low air flow setting. This is due to the greater impact of systematic errors that are commonly exhibited at the lower flow ranges of the instrumentation. However, these differences

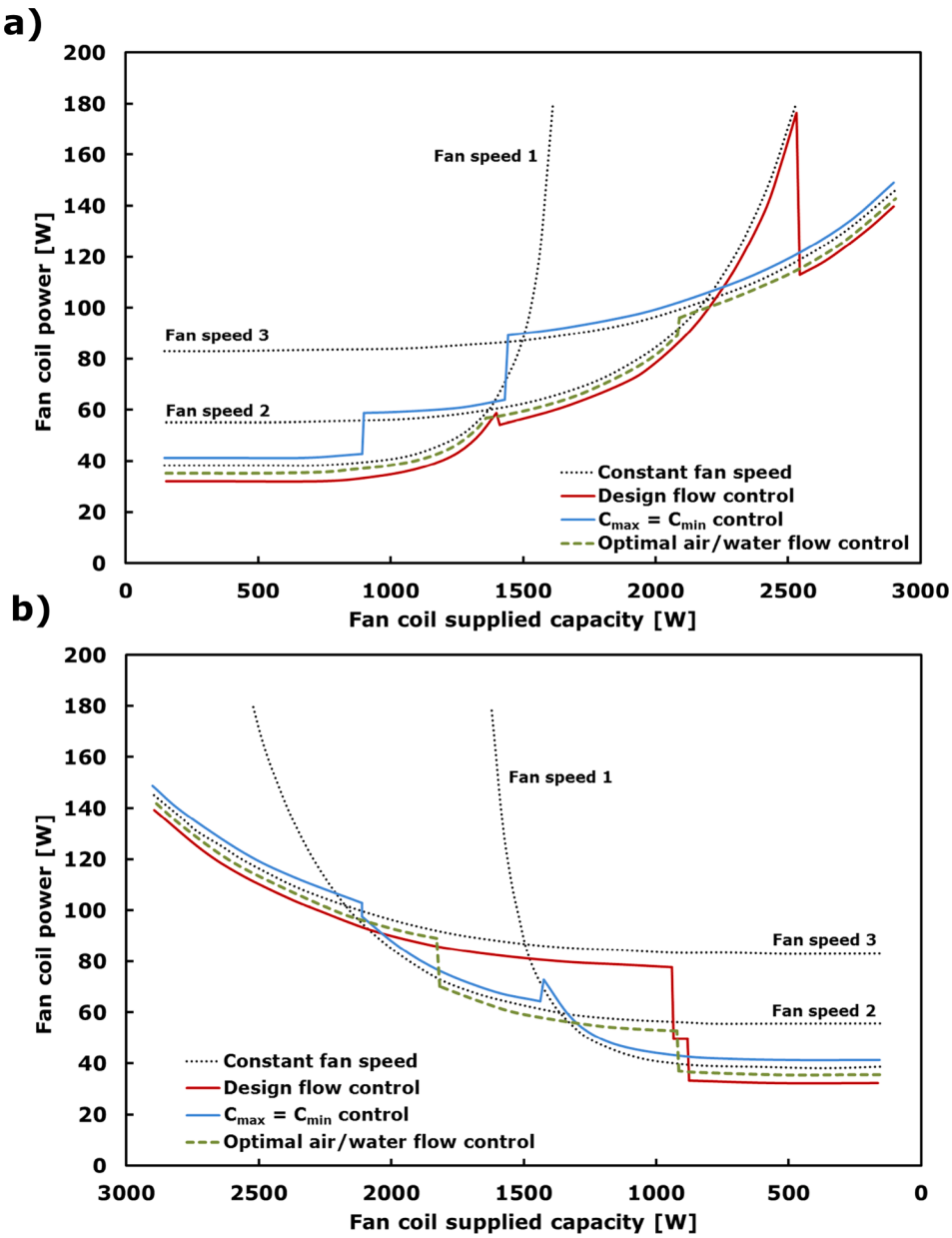

Fig. 8. Total fan coil power VS supplied capacity for bypass fan coil battery. a) Increasing fan coil capacity. b) Decreasing fan coil capacity.

are always less than 10%, which is considered acceptable as per ASHRAE standard [36] and other research [37,38], especially considering the simplified nature of the correlation adopted. Therefore, the proposed correlation was deemed to be sufficiently capable of estimating fan coil capacity across the three speed settings.

2.3.3. Strategy development

Since the fan coil capacity and the power consumption can be calculated from design data and from measured fan speed and water flow rates, it is possible to develop a control strategy aimed at minimising the fan coil battery power consumption by determining the optimal air/water flow rate. As mentioned earlier, this optimum can only be calculated by considering all fan coils, as the pump power is dependent on the flow through each coil. If a building has N fan coil units, each with 3 fan speeds, 3^N possible combinations exist, making the iterative process too expensive to be computed. Notwithstanding, the optimisation can be greatly simplified by setting fan speed based on the relative fan coil loads.

Fig. 7 illustrates the optimisation procedure adopted in the present work. Starting from the fan speed and water flow rated measurements (Step 1 and 2), the required capacity of each zone is obtained (Step 3), then the total power consumption is calculated with all fans at the same speed (Step 4). Subsequently, water flow rates are then calculated for all 3 fan speeds available at a fixed capacity input (Step 5). As described in Section 2, the water flow rate is modulated through PID control to maintain room temperature at the set-point. Therefore, the supplied load will equal the zone load demand. The zone load can therefore be calculated directly using the fan coil capacity equations (Eq. 6 and Eq. 7) for the specific fan speed, from knowledge of the water flow rate, which can be estimated from the total battery water flow rate and the valve position in each unit.

The capacity equations for all fan speeds can then be solved iteratively (Step 6, Fig. 7), using the zone capacity as an input and calculating the corresponding water flow rate in each condition. The three sets of water flow rate and fan speed combinations supplying the required capacity are used to calculate pump and fan powers for each case. By setting the fan speed to the optimal set-point, the water flow rate is automatically adjusted as a result of PID control. Therefore, the fan

speed set-point is the only output from this strategy. As the inlet air and water temperature are not affected by a change in fan speed the zone load, which is calculated using the capacity equation, it does not need to be adjusted for actual inlet temperatures. Therefore, only the fan speed and water flow rate are required as inputs.

Finally, the proposed algorithm is assumed to be independent of sensor response time, as the algorithm controlled output, i.e., the fan speed, is maintained at a fixed speed for a number of minutes at a time. Accordingly, the instrument time response characteristics are considered to be negligible, in what is in essence a form of quasi-steady state form of control. The robustness of this assumption is left as a future research question.

3. Results

The optimal air/water flow control strategy was analysed assuming steady state and quasi-steady state conditions for a range of thermal loads. Steady state analysis was performed to evaluate the strategy over the full range of possible building loads, while quasi-state analysis was implemented to demonstrate the performance over expected daily building load profiles. For each strategy, the water flow rate was controlled to maintain room air temperature at the set-point through built-in water flow control and a fixed inlet water temperature of 7 °C in cooling was selected. Strategies were evaluated for both increasing and decreasing building capacities. This was done because the fan speed selected by a strategy, at a given capacity, is dependent on whether a higher or lower capacity was recorded in the previous time step. Both by-pass and modulated valve fan coil battery models, with fixed inlet water temperature, have been analysed. In both cases, the optimal strategy is compared to nominal fan speed operation and the benchmark strategies, which were described in Section 2. For nominal operation, a fixed fan speed of 3 was selected for each zone to ensure that the required load was supplied.

The following sections report the results obtained by the steady state (Section 3.1) and by the quasi-steady state analyses for the developed control strategies.

3.1. Steady state analysis

3.1.1. Bypass fan coil battery

In case of using a bypass fan coil battery, a single fan coil can be studied in isolation, as the water flow is assumed to be divided equally between the fan coils. The total fan coil power is equal to the sum of the pump power and fan power for one coil. The total fan coil power resulting from each strategy is shown in Fig. 8a, for increasing supplied fan coil capacities, and in Fig. 8b, for decreasing capacities.

For a given supplied capacity, three possible combinations of fan speeds and water flow rates are available. One of these combinations results in the lowest total fan coil power. If the capacity increases (Fig. 8a), optimal fan speed control will result in near-optimal fan speeds over the full capacity range. $C_{min} = C_{max}$ control shows an increment of fan speeds at low capacity values, resulting in a higher total power (up to 27 W above the optimum) for zone loads between 900 and 2250 W due to excessive fan power. A low total power is observed for the majority of evaluated capacities in case of design flow control. However, fan speed is not increased appropriately for capacity values above 2300 W, resulting in a higher total power.

For decreasing capacities (Fig. 8b), optimal fan speed control does not operate as effectively as observed for increasing capacities. Fan speeds are not reduced optimally, resulting in marginally higher total power values for a small range of capacities (up to 20 W above the optimum). This is due to simplifications made when deriving the fan coil capacity equation and the circulation pump control model. $C_{min} = C_{max}$ control results in the lowest total power of all evaluated strategies for low capacities. However, this strategy is observed to perform poorly for increasing capacities. A high total power is evident for design flow control (up to 80 W above the optimum) over a significant range of capacities. This control specifies a reduction in fan speed when a low flow limit is reached, which results in high fan speeds for decreasing capacity values. Overall, for increasing and decreasing capacities, optimal fan speed control results in the lowest total fan coil power.

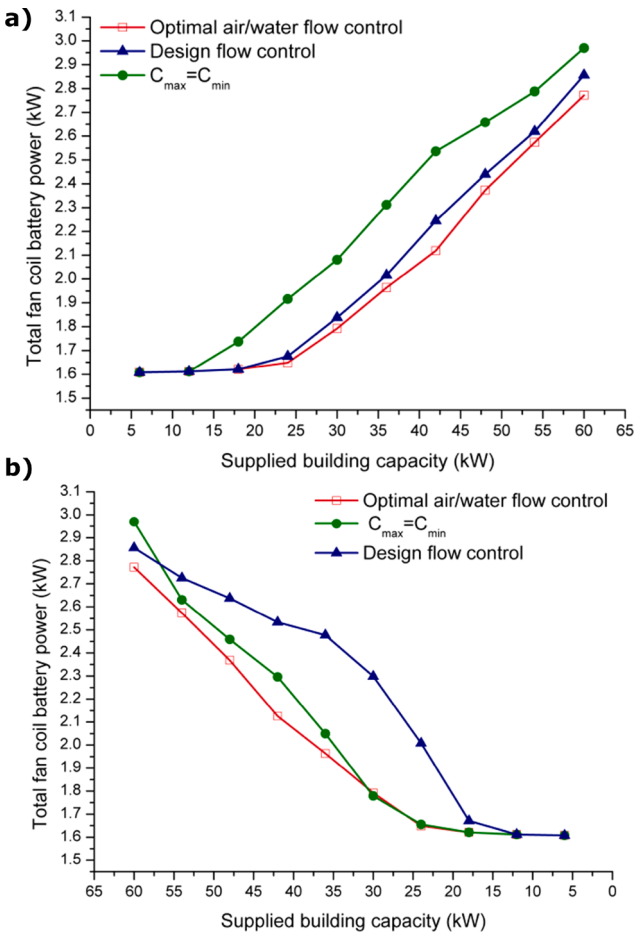

Fig. 9. Total fan coil battery power VS supplied capacity for bypass fan coil battery. a) Increasing fan coil capacity. b) Decreasing fan coil capacity.

3.1.2. Modulated fan coil battery

In case of valve modulation of fan coil batteries, one fan coil cannot be evaluated in isolation since the pump power is dependent on the flow through each of the zones, which varies according to individual zone loads. Therefore, a simulation of the full battery sub-system is required. The fan coil battery model was simulated over a range of increasing (Fig. 9a) and decreasing (Fig. 9b) building loads, with a fixed inlet water temperature. The total fan coil battery power consumption consists of the combined total fan power and the circulation pump power. $C_{min} = C_{max}$ control showed the highest total fan coil battery power consumption for all increasing capacities, noting that it performed more effectively for lower values. Conversely, design flow control showed a lower total power consumption for increasing capacities, and the highest total power for decreasing capacities. Over the full range of increasing and decreasing supplied building loads, optimal fan speed control demonstrated the minimum total fan coil battery power consumption.

For all capacities, an average reduction in total power of 5.7% and 5.9% is observed when optimal fan speed control is compared with $C_{min} = C_{max}$ control and design flow control, respectively. The saving increases up to 29% when compared to a constant fan speed setting of 3 in all zones. For building loads below 15 kW, no difference in total power is recorded for the evaluated strategies.

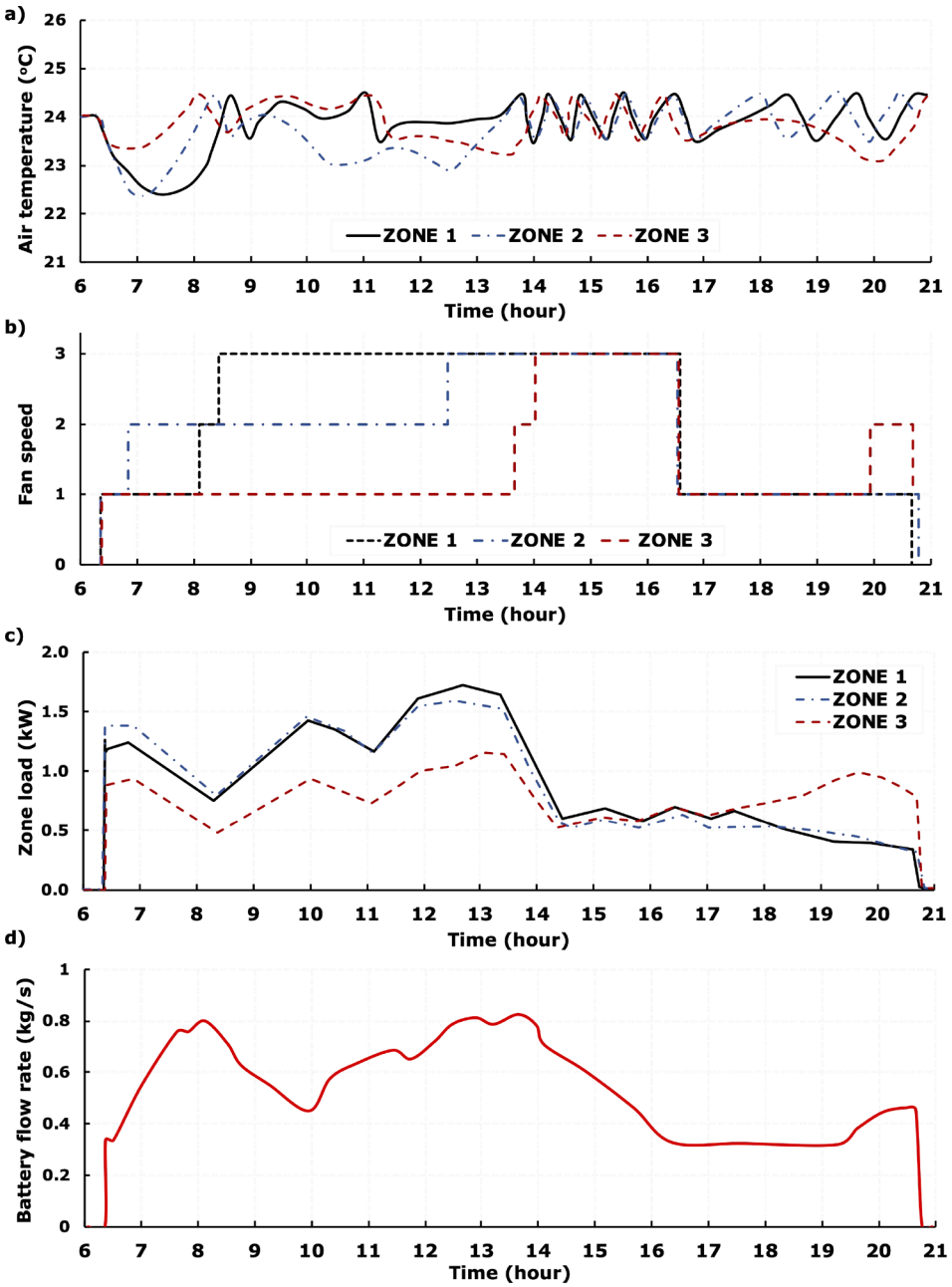

Fig. 10. Daily simulation profile, bypass fan coil battery and optimal fan speed control: a) Zone air temperature; b) Fan speed; c) Zone load and d) Battery flow rate.

3.2. *Quasi-steady state analysis*

Optimal fan speed control, $C_{min} = C_{max}$ control and design flow control were evaluated for quasi-steady state conditions, with a resolution of 1 min, using the simulation models developed. The total daily energy consumption of the fan coil batteries, using each strategy, was then calculated for each of the simulation days.

3.2.1. *Bypass fan coil battery*

Fig. 10 shows the battery water flow rate along with fan speeds, room air temperatures and loads of three building zones (Z1, Z2, Z3) for the same simulation day. At 6:30 am water flow control is set to maintain room air temperature in zone 2 at the set-point, as the air temperature has exceeded the lower PID bandwidth. The water flow rate increased after this point to match the zone load. Optimal fan speed control is activated at 7 am, which results in an increase in fan speed setting in zone 2, from speed 1 to speed 2. Water flow rate control switches to zone 1 at 8:00 am and the fan speed is increased to speed 2, then speed 3, due to optimal fan speed control. As the air temperature in zone 1 increases, the water flow rate begins to decrease. At 8:40 am, the water flow rate continues to decrease as no zone is under control. At 12:15 pm, control switches to zone 2, resulting in a steady increase in water flow rate.

Optimal fan speed control results in an increase in zone 2 fan speed, from setting 2 to setting 3. Water flow control is set to zone 3 at 1:30 pm, and fan speed is increased to setting 3. Beyond this, all zone temperatures cycle due to a reduction in building load. As a result, the water flow rate decreases gradually until the minimum flow limit is reached. The fan speed in all zones is reduced to 1 at 4:30 pm, as no room temperature has exceeded the PID bandwidth. The water flow rate increases at 8 pm, to maintain room air temperature in zone 3, and the fan speed is increased to setting 2, as a result of optimal fan speed control.

The resulting total daily fan coil battery energy for all simulated days are reported in Figs. 11a and b, for heating and cooling conditions respectively. In heating mode, optimal fan speed control results in a

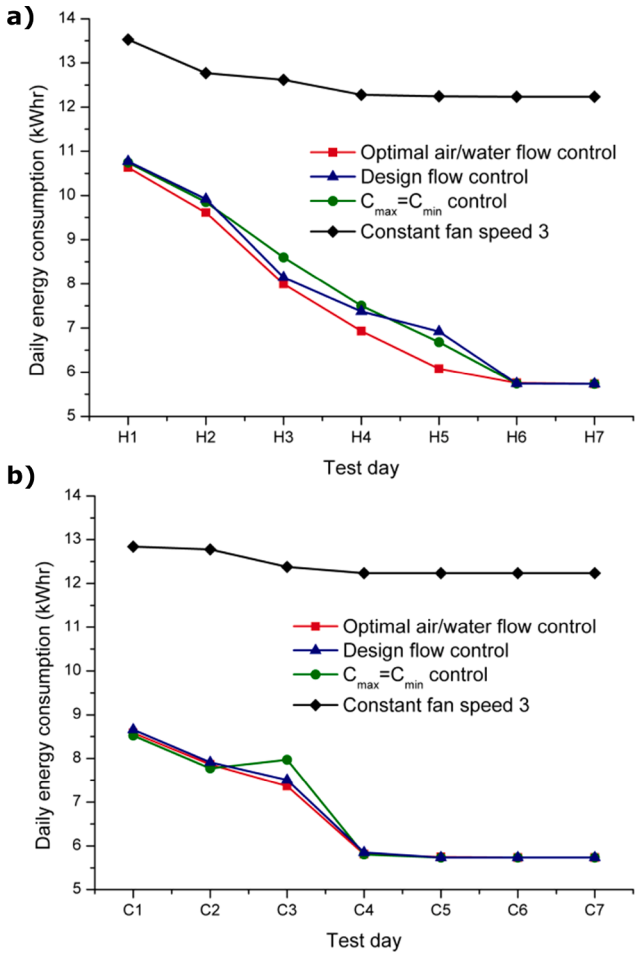

Fig. 11. Heating (a) and cooling (b) daily fan coil battery energy usage. Bypass fan coil battery.

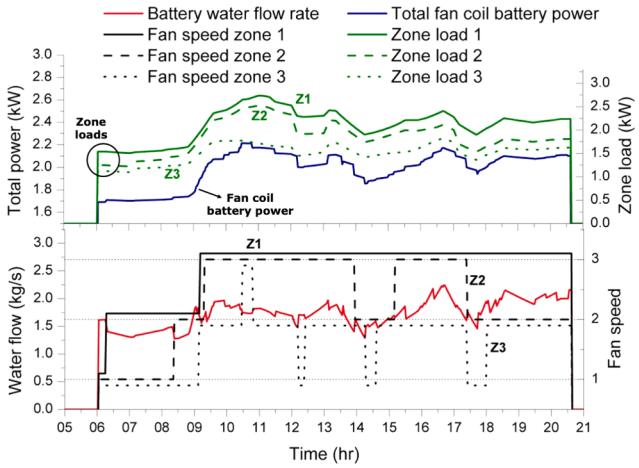

Fig. 12. Daily simulation profile, bypass fan coil battery and optimal fan speed control.

lower total daily energy usage than the other evaluated strategies for all days. An average reduction in total energy of 5.4% and 4.9% is observed when compared to $C_{min} = C_{max}$ control and design flow control, respectively. For the cooling season, a negligible difference in energy consumption is observed when implementing optimal fan speed control, $C_{min} = C_{max}$ control and design flow control.

For low thermal loads (simulation days H6, H7, C4-C7), no difference

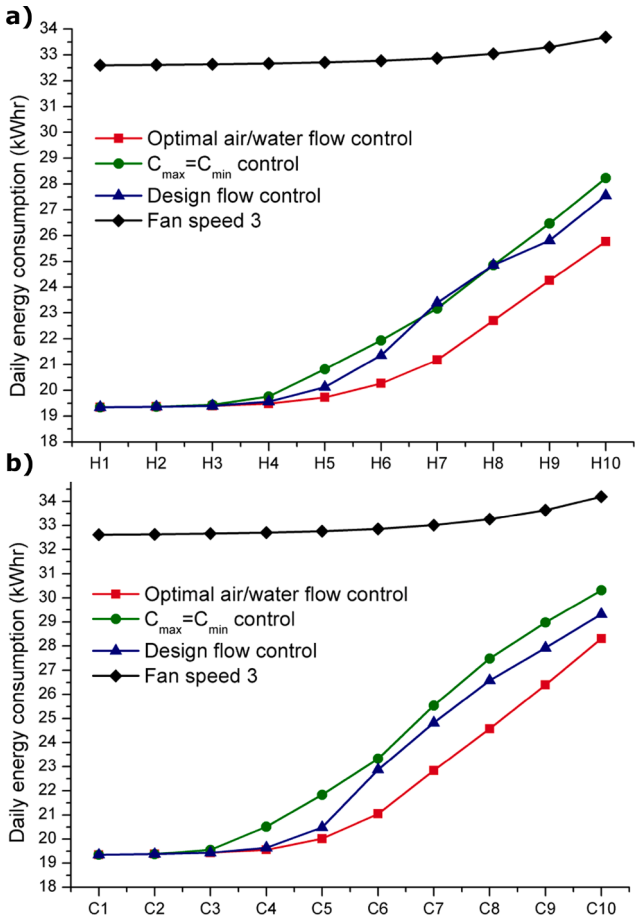

Fig. 13. Heating (a) and cooling (b) daily fan coil battery energy usage. Modulated valve fan coil battery.

in total energy is observed between the evaluated fan speed control strategies, since all fan speeds are at setting 1 regardless of the implemented strategy. However, the use of optimal control showed a significant reduction of energy consumption for both heating (approximately 35%) and cooling (approximately 43%), if compared to adopting the maximum fan speed setting in all zones.

3.2.2. *Modulated fan coil battery*

Fig. 12 shows the optimal fan speed control in operation for a sample cooling day. Building load, total fan coil battery power consumption and battery water flow rate profiles are displayed along with the fan speed settings in 3 of the zones. For this system, optimal fan speed control operates to reduce total fan and pump power through control of all fans. Built-in water flow control ensures room air temperature is continuously maintained in each zone. For increasing load, observed at 10 am, 1:30 pm, 4:30 pm, and 7:00 pm, an increase in fan speed is noted, due to optimal fan speed control. The fan speed selected is dependent on the specific zone load, which results in higher fan speeds being selected for higher zone loads. The fan speed in zones 2 and 3 decrease when a decrease in zone load is observed at 12:30 pm, 2:00 pm and 5:30 pm.

Figs. 13a and b show the simulated total daily energy consumption for the modulated valve fan coil battery for all evaluated control strategies in heating and cooling. As with the bypass fan coil battery subsystem, no difference in total energy is observed between the evaluated strategies for low load days. This is due to the minimum speed setting being selected for all fans. Optimal fan speed control results in the minimum total energy consumption for all simulated days in heating and cooling, when compared to the other evaluated strategies. A high base energy consumption is observed (19.5 kWh), which is primarily

Table A.2
Parameters calculation [32].

Parameter	Unit
$K_{d1} = \frac{h_{w,d}A_{w,d}}{h_{a,d}A_{a,d}}$	–
$K_{d2} = \Delta T_{a,d}$	°C
$K_{d3} = \Delta T_{w,d}$	°C
$K_{d4} = \theta_d$	°C
$K_{d5} = \frac{K_{d2}}{K_{d4}}$	–
$K_{d6} = \frac{K_{d3}}{K_{d4}}$	–

comprised of fan energy consumption. Optimal fan speed control results in a maximum reduction in energy usage of 7.9% and 9.1%, when compared to $C_{min} = C_{max}$ control in heating and cooling, respectively. A maximum reduction of 6.3% and 5.8% is observed when compared to design flow control in heating and cooling, respectively. On average total energy is reduced by 34% when optimal fan speed control is used over maximum fan speed settings in each zone.

4. Conclusions

A control strategy for controlling air and water flow rates to optimise fan coil battery performance is presented. Due to differences in fan coil battery design, separate strategies are developed for bypass and modulated valve fan coil battery sub-systems. However, both strategies are developed using the same principles. The optimal fan speed control strategy was developed through derivation and implementation of a fan coil capacity estimation equation and a circulation pump power control model. The developed control uses a reduced number of input parameter and it was compared to other control strategies in steady state and quasi-steady state operation. The results showed that the optimisation strategy operates effectively under a range of loads and is applicable to different system designs requiring only readily available inputs. The main outcomes obtained can be summarised as follows:

- Optimal fan speed control results in the minimum daily energy consumption for the bypass fan coil battery in heating mode, while similar daily energy values are recorded for all fan speed control strategies. This is due to differences in the building load profiles for heating and cooling. Savings of between 4.9% and 5.4% can be achieved by the optimal fan speed control if compared with the other control strategies.
- For the modulated valve fan coil battery operating in quasi-steady state, optimal fan speed control results in the lowest total energy values of all evaluated strategies, allowing savings between 7.9% and 9.1% if compared with the other control strategies.
- Energy savings obtained by using optimal fan speed control are greater than those reported for the bypass value battery, as the control strategy operates on all fans in the sub-system.
- Similar energy consumption values are observed when implementing the fan speed control strategies for days with low loads, as all fan are set to speed 1 regardless of strategy used.
- Significant savings (up to 34% in heating mode and up to 43% in cooling mode) are reported when any of the fan speed control strategies are compared to fixed fan speed operation.

The prospects for the optimisation strategy outlined in the current paper lie in the generality and operational application simplicity of the proposed approach, as only a single real time measurement is required (i.e., the water mass flowrate for a fan coil battery), plus fan speed and water valve settings for each fan coil. Any approach that reduces the amount of active measured data leads to more reliable operation despite less data availability, as it results in a lower probability of malfunctioning instrumentation and associated data errors. Therefore, in large fan coil battery systems, such as the one examined in the current work, the proposed approach has potential: (i) to ameliorate data error by using minimal instrumentation instances, (ii) to reduce associated instrument capital costs, and, (iii) to enhance system savings arising from the proposed algorithm.

Limitations of the current contribution is that the original mathematical model has been validated for a smaller heat pump and fan battery systems as described in [14,30,31]. The adaptation in the current work involves a larger, albeit similar heat pump system, with additional number of fan coil units in the battery system. Further work would include testing the proposed algorithms in field system trials, examining the effectiveness of the control algorithms, which is left as future work.

Declaration of Competing Interest

The authors declare that they have no known competing financial interests or personal relationships that could have appeared to influence the work reported in this paper.

Acknowledgement

This work has emanated from research conducted with the financial support of the European Commission, 7*th* Framework Programme (Grant Agreement: TREN/FP7EN/218895).

Appendix A. Fan coil correlations for heating and cooling modes

Markusson et al. [32] developed a correlation (Eq. A.1) to express the fan coil capacity y (Eq. 4) as function of the change in water flow rate x (Eq. 5), assuming a fixed fan speed.

$$y = \frac{F(x)(1 + K_{d5} + K_{d6})x}{x + F(x)(xK_{d5} + K_{d6}} \tag{A.1}$$

$$F(x) = x^m \frac{1 + K_{d1}}{1 + K_{d1}x^m} \tag{A.2}$$

The parameters in Eq. A.1 and Eq. A.2 can be calculated as shown in Table A.2.

A new correlation has been developed in order to express Eq. A.1 as function of the inlet temperatures only. Considering a general formulation for a heat transfer process (Eq. A.3), the definition of *y* provided in Eq. 4, can be rewritten as shown in Eq. A.4.

$$Q = UA\theta \tag{A.3}$$

$$y = \frac{Q_r}{Q_d} = \frac{(UA)_r\theta_r}{(UA)_d\theta_d} = \frac{\frac{1}{(UA)_d}\theta_r}{\frac{1}{(UA)_r}\theta_d} \tag{A.4}$$

The terms r and d in Eq. A.4 represent the required and design value respectively, while θ represents the mean temperature difference defined as follows:

$$\theta = \frac{\left(T_{w,in} - T_{w,out}\right) - \left(T_{a,in} - T_{a,out}\right)}{2} \tag{A.5}$$

The UA value can be simplified by neglecting the heat exchanger thermal conduction resistance [39]:

$$\frac{1}{UA} = \frac{1}{h_w A_w} + \frac{1}{h_a A_a} \tag{A.6}$$

As the fan speed is fixed, the design and required air convective heat transfer coefficients are equivalent. Therefore:

$$h_{a,r} = h_{a,d} = h_a \tag{A.7}$$

$$y = \frac{\left(\frac{1}{h_{w,d}A_w} + \frac{1}{h_a A_a}\right)\theta_r}{\left(\frac{1}{h_{w,r}A_w} + \frac{1}{h_a A_a}\right)\theta_d} = \frac{\left(1 + \frac{h_{w,d}A_w}{h_a A_a}\right)\theta_r}{\left(\frac{h_a A_a}{h_{w,r}A_w} + \frac{h_{w,d}A_w}{h_a A_a}\right)\theta_d} \tag{A.8}$$

The water heat transfer coefficient is assumed to be proportional to the flow rate raised to an exponent m, using the Wilson plot method for fully developed turbulent flow inside a circular tube [40].

$$h_w = C_w \dot{m}_w^m x^m \tag{A.9}$$

Using the above definition, the ratio $h_{w,r}/h_{w,d}$ can be written as shown below:

$$\frac{h_{w,r}}{h_{w,d}} = \left(\frac{\dot{m}_{w,r}}{\dot{m}_{w,d}}\right)^m = x^m \tag{A.10}$$

Therefore:

$$y = \frac{\left(1 + \frac{h_{w,d}A_w}{h_a A_a}\right)\theta_r}{\left(\frac{1}{x^m} + \frac{h_{w,d}A_w}{h_a A_a}\right)\theta_d} \tag{A.11}$$

Introducing the term $F(x)$, defined as Eq. A.13, the following expression can be obtained.

$$y = F(x)\frac{\theta_r}{\theta_d} \tag{A.12}$$

$$F(x) = \frac{x^m\left(1 + \frac{h_{w,d}A_w}{h_a A_a}\right)}{1 + \frac{h_{w,d}A_w}{h_a A_a}x^m} \tag{A.13}$$

The mean temperature difference (θ), Eq. A.5, can be easily calculated for the design case (θ_d). However, the outlet air and water temperatures for the required case are unknown. In order to determine θ_r, the outlet temperatures are expressed as a function of x, y and the design temperatures. Considering the definition given for y (Eq. 4), we have:

$$y = \frac{Q_r}{Q_d} = \frac{\dot{m}_{w,r}c_{p,w}\Delta T_{w,r}}{\dot{m}_{w,d}c_{p,w}\Delta T_{w,d}} = x\frac{\Delta T_{w,r}}{\Delta T_{w,d}} \tag{A.14}$$

Therefore:

$$\Delta T_{w,r} = \frac{y}{x}\Delta T_{w,d} \tag{A.15}$$

$$\Delta T_w = T_{w,in} - T_{w,out} \tag{A.16}$$

$$T_{w,out,r} = T_{w,in} - \frac{y}{x}\Delta T_{w,d} \tag{A.17}$$

The same procedure can be applied to the air side, in order to obtain the following:

$$T_{a,out,r} = T_{a,in} + y\Delta T_{a,d} \tag{A.18}$$

Substituting Eq. A.17 and Eq. A.18 into Eq. A.5, the following expression can be obtained:

$$\theta_r = \left(T_{w,in} - T_{a,in}\right) + \frac{y}{2}\left(\frac{T_{w,out,d} - T_{w,in}}{x} + T_{a,in} - T_{a,out,d}\right) \tag{A.19}$$

Finally, substituting Eq. A.19 into Eq. A.12, the final correlations for heating (Eq. 6) and cooling (Eq. 7) can be obtained.

References

[1] European Council, Directive 2010/31/eu of the european parliament and of the council of 19 may, 2010 on the energy performance of buildings, Official Journal of the European Union, 2010.
[2] European Council, Directive 2012/27/eu of the european parliament and of the european council, Official Journal of the European Union 2012.
[3] M. Carragher, M. De Rosa, A. Kathirgamanathan, D.P. Finn, Investment analysis of gas-turbine combined heat and power systems for commercial buildings under different climatic and market scenarios, Energy Convers. Manage. 183 (2019) 35–49.
[4] M. Castilla, J. Bonilla, J. Álvarez, F. Rodríguez, A room simulation tool for thermal comfort control in a bioclimatic building: A real example of use with an optimal controller, Opt. Contr. Appl. Methods 37 (2016) 479–495.
[5] Japan Refrigeration and Air Conditioning Industry Association (JRAIA), World Air Conditioner Demand by Region, Technical Report, JRAIA, 2019.
[6] G.P. Henze, A.G. Floss, Evaluation of temperature degradation in hydraulic flow networks, Energy Build. 43 (2011) 1820–1828.
[7] X. Li, T. Zhao, J. Zhang, T. Chen, Development of network control platform for energy saving of fan coil units, J. Build. Eng. 12 (2017) 155–160.
[8] F. Pallonetto, M. De Rosa, D.P. Finn, Environmental and economic benefits of building retrofit measures for the residential sector by utilizing sensor data and advanced calibrated models, Adv. Build. Energy Res. (2020) 1–29.
[9] X. Jin, Z. Du, X. Xiao, Energy evaluation of optimal control strategies for central vwv chiller systems, Appl. Therm. Eng. 27 (2007) 934–941.
[10] Z. Tianyi, Z. Jili, S. Dexing, Experimental study on a duty ratio fuzzy control method for fan-coil units, Build. Environ. 46 (2011) 527–534.
[11] A. Martinčević, M. Vašak, V. Lešić, Identification of a control-oriented energy model for a system of fan coil units, Control Eng. Pract. 91 (2019) 104100.
[12] G. Wang, L. Song, Air handling unit supply air temperature optimal control during economizer cycles, Energy Build. 49 (2012) 310–316.
[13] F. Karlsson, P. Fahlén, Capacity-controlled ground source heat pumps in hydronic heating systems, Int. J. Refrig. 30 (2007) 221–229.
[14] J. Corberan, D. Finn, C. Montagud, F. Murphy, K. Edwards, A quasi-steady state mathematical model of an integrated ground source heat pump for building space control, Energy Build. 43 (2011) 82–92.
[15] C.-M. Lin, H.-Y. Liu, K.-Y. Tseng, S.-F. Lin, Heating, ventilation, and air conditioning system optimization control strategy involving fan coil unit temperature control, Appl. Sci. 9 (2019) 2391.
[16] A. Martincevic, M. Vašak, V. Lešic, Identification of a control-oriented energy model for a system of fan coil units, Control Eng. Pract. 91 (2019) 104100.
[17] X. Xu, Z. Zhong, S. Deng, X. Zhang, A review on temperature and humidity control methods focusing on air-conditioning equipment and control algorithms applied in small-to-medium-sized buildings, Energy Build. 162 (2018) 163–176.
[18] Z. Ma, S. Wang, An optimal control strategy for complex building central chilled water systems for practical and real-time applications, Build. Environ. 44 (2009) 1188–1198.
[19] M. Teitel, A. Levi, Y. Zhao, M. Barak, E. Bar-lev, D. Shmuel, Energy saving in agricultural buildings through fan motor control by variable frequency drives, Energy Build. 40 (2008) 953–960.
[20] S. Kakac, H. Liu, A. Pramuanjaroenkij, Heat exchangers: selection, rating, and thermal design, CRC Press, 2020.
[21] P. Fahlén, H. Voll, J. Naumov, Efficiency of pump operation in hydronic heating and cooling systems, J. Civ. Eng. Manage. 12 (2006) 57–62.
[22] M.-T. Ke, K.-L. Weng, C.-M. Chiang, Performance evaluation of an innovative fan-coil unit: Low-temperature differential variable air volume fcu, Energy Build. 39 (2007) 702–708.
[23] H. Madani, J. Claesson, P. Lundqvist, A descriptive and comparative analysis of three common control techniques for an on/off controlled ground source heat pump (gshp) system, Energy Build. 65 (2013) 1–9.
[24] X. Zhang, C. Yu, S. Li, Y. Zheng, F. Xiao, A museum storeroom air-conditioning system employing the temperature and humidity independent control device in the cooling coil, Appl. Therm. Eng. 31 (2011) 3653–3657.
[25] Y. Nam, R. Ooka, Numerical simulation of ground heat and water transfer for groundwater heat pump system based on real-scale experiment, Energy Build. 42 (2010) 69–75.
[26] P. Fahlén, C.H. Stignor et al., Capacity control of liquid-cooled air-coolers, in: The 22nd International Congress of Refrigeration, pp. A-X.
[27] C. Markusson, Efficiency of building related pump and fan operation-Application and system solutions, Chalmers University of Technology, 2011.
[28] GROUNDMED, Dg: Tren/fp7en/218895, European 7th Framework Programme, 2017.
[29] A.D. Carvalho, P. Moura, G.C. Vaz, A.T. de Almeida, Ground source heat pumps as high efficient solutions for building space conditioning and for integration in smart grids, Energy Convers. Manage. 103 (2015) 991–1007.
[30] K. Edwards, D. Finn, Generalised water flow rate control strategy for optimal part load operation of ground source heat pump systems, Appl. Energy 150 (2015) 50–60.
[31] C. Montagud, J.M. Corberán, F. Ruiz-Calvo, Experimental and modeling analysis of a ground source heat pump system, Appl. Energy 109 (2013) 328–336.
[32] C. Markusson, L. Jagemar, P. Fahlén, Energy recovery in air handling systems in non-residential buildings-design considerations, ASHRAE Trans. 116 (2010) 154.
[33] IMST-ART, Simulation tool to assist the selection, design and optimization of refrigerator equipment and components, Universitat Politècnica de Valéncia, Instituto de Ingenieria Energética, Spain, 2020.
[34] K.C. Edwards, Generalised integrated control strategies for optimal control of media flow rates in ground source heat pump systems for maximising seasonal performance factor (PhD Thesis), University College Dublin, 2014.
[35] K.C. Edwards, D. Finn, Air and water flow rate optimisation for a fan coil unit in heat pump applications, in: International High Performance Buildings Conference at Purdue, July 16–19, 2012, Purdue University, 2012.
[36] A. Guideline et al., Measurement of energy, demand, and water savings, in: ASHRAE Guidel 14-2014, 2014.
[37] G.R. Ruiz, C.F. Bandera, Validation of calibrated energy models: Common errors, Energies 10 (2017) 1587.
[38] V. Gutiérrez González, G. Ramos Ruiz, C. Fernández Bandera, Empirical and comparative validation for a building energy model calibration methodology, Sensors 20 (2020) 5003.
[39] F.C. McQuiston, J.D. Parker, J.D. Spitler, Heating, ventilating, and air conditioning: analysis and design, John Wiley & Sons, 2004.
[40] J. Fernandez-Seara, F.J. Uhía, J. Sieres, A. Campo, A general review of the wilson plot method and its modifications to determine convection coefficients in heat exchange devices, Appl. Therm. Eng. 27 (2007) 2745–2757.